Nonlinear optics
$\chi^{(2)}$ MATERIALS

0.1 Nonlinear optics in $\chi(2)$ media

In this section, we will only focus on materials which present a nonlinear susceptibility $\chi^{(2)}$. As we saw from the previous chapter, this happens in the case of the Lorentz model with an asymmetric potential. Fig. 1 presents the linear (blue curve) and nonlinear (red curve) response of polarization $\mathbf{P}$ to an applied field $\mathbf{E}$. As a field propagates in a $\chi^{(2)}$ material, not only it will induce such polarization, but the polarization will then act back on the field itself. The modified field $\mathbf{E}_{\text{out}}$ is also presented.

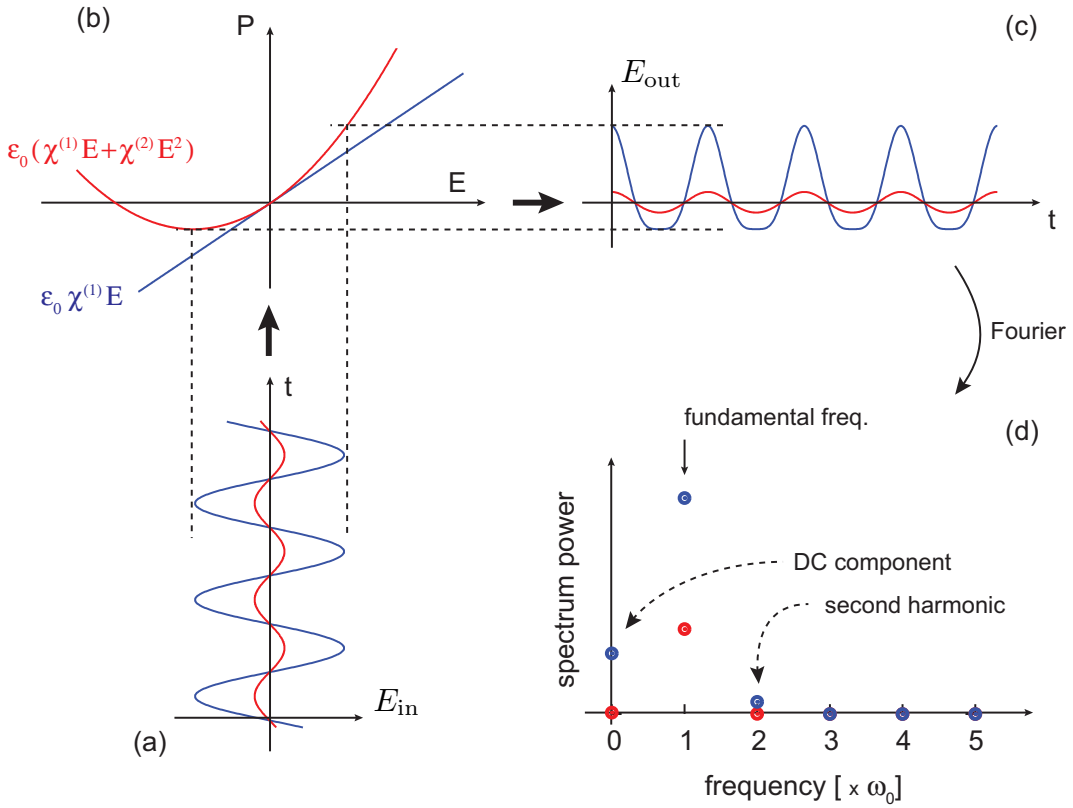

Figure 1: Effect of the induced polarization on the electric field for low (red) and high (blue) input power in a $\chi^{(2)}$ material. For high input power, the Fourier spectrum shows the appearance of a component at $2\omega_0$ (second harmonic) as well as a DC component.

From the power spectrum of the output field (Fig. 1-d), we can see that as the strength of the input field increases (blue curve), new components appear in the spectrum:

1. a DC-component
2. a component at the second harmonic

Actually, $\chi^{(2)}$ materials can be used for the following nonlinear applications:

1. three waves mixing

2. second harmonic generation
3. sum and difference frequencies generation
4. parametric oscillation

0.1.1 Frequency mixing

Let's assume that we have two fields entering a $\chi^{(2)}$ material. The field is simply the superposition of two simple electric fields:

$$E = E_1 e^{i\omega_1 t} + E_2 e^{i\omega_2 t} + c.c. \tag{1}$$

and the induced polarization:

$$P = \epsilon_0 \chi^{(2)} \left[E_1 e^{i\omega_1 t} + E_2 e^{i\omega_2 t} + c.c. \right]^2 \tag{2}$$

After calculation, the polarization is:

$$\begin{aligned}
P = \quad & \epsilon_0 \chi^{(2)} \left(E_1^2 e^{2i\omega_1 t} + c.c. \right) && \leftarrow \text{ SHG of } E_1 \\
+ \ & \epsilon_0 \chi^{(2)} \left(E_2^2 e^{2i\omega_2 t} + c.c. \right) && \leftarrow \text{ SHG of } E_2 \\
+ \ & 2\epsilon_0 \chi^{(2)} \left(E_1 E_2 e^{i(\omega_1+\omega_2)t} + c.c. \right) && \leftarrow \text{ sum frequency } (\omega_1 + \omega_2) \\
+ \ & 2\epsilon_0 \chi^{(2)} \left(E_1 E_2^* e^{i(\omega_1-\omega_2)t} + c.c. \right) && \leftarrow \text{ difference frequency } (\omega_1 - \omega_2) \\
+ \ & \epsilon_0 \chi^{(2)} \left(|E_1|^2 + |E_2|^2 \right) && \leftarrow \text{ DC field : optical rectification}
\end{aligned}$$

Of course, for each case, the input field generates a polarization, which drives the field component through Maxwell's equations. At that moment, the important question to ask is : *"Will we generate all these frequencies as soon as we use 2 fields in a $\chi(2)$ materials?"*. The answer is *fortunately* <u>*no*</u>.

0.1.2 Franken's experiment of second harmonic generation

One of the most famous paper in nonlinear optics is certainly the 1^{st} demonstration of the generation of second harmonic in quartz by Franken, Hill, Peter and Weinreich in 1961. In this experiment, the authors used a recently demonstrated ruby laser ($\lambda_p = 0.694\ \mu$m), operating in pulsed regime. The laser beam is focused into a quartz crystal and the output beam (pump & second harmonic) was dispersed with a prism and sent onto a photographic plate (fig. 2).

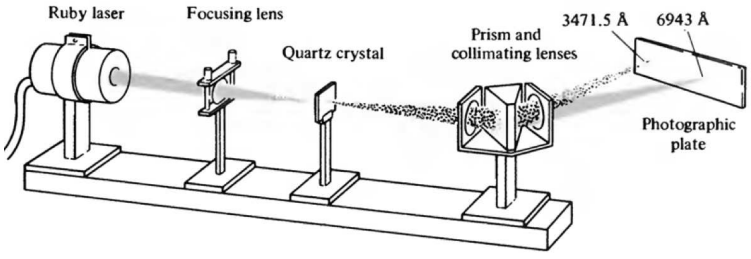

Figure 2: Experimental setup of the Franken's experiment of second harmonic generation.

This paper is not only famous for the amazing result that was presented: it was indeed the very first time that someone could demonstrate that a coherent source (laser beam) could lead to the generation of coherent harmonics, and this was clearly an important milestones for optics. This paper is also famous because, the result does not appear in

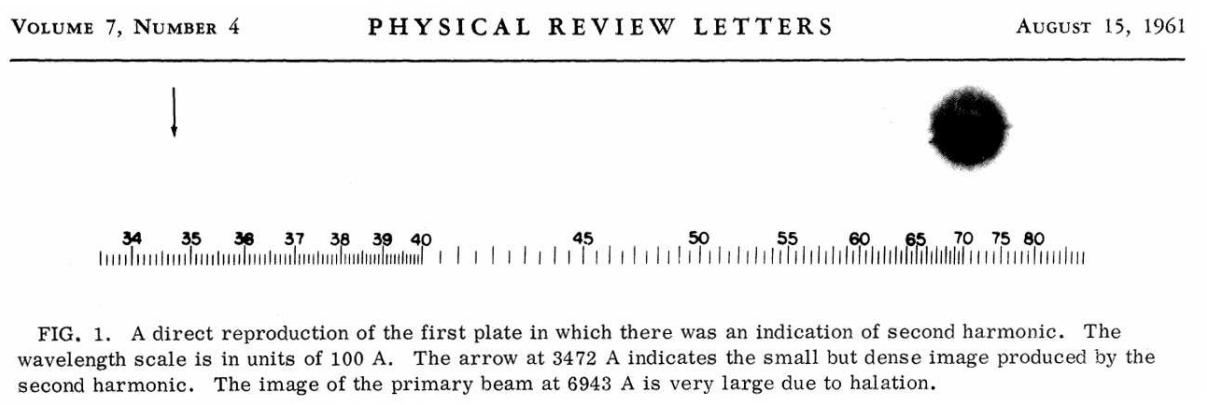

Figure 3: Copy of the figure from presenting the results of the second harmonic generation by the group of P. Franken in 1961.

the paper! As you can see on the copy of the main figure of that paper (fig. 3), published in *Physical Review letter* in 1961, the arrow, supposed to point at the second harmonic, does not point to anything! At that time, the authors could not simply send a pdf version of their paper, including high-resolution figures and check the proofs of the paper just before its publication on the web! Actually, the final stage was to go through a printer, who was preparing the new edition of PRL. But the conversion efficiency of the process was so low ($\simeq 10^{-8}$ conversion efficiency) that the result, a small point caught by the photographic plate, was considered as a simple dust by the editor, who simply erased it!

Let's see why the conversion efficiency of the original second harmonic experiment was so small. The input field is simply

$$E_1 = A_1 \cos(\omega_1 t - k_1 z) \tag{3}$$

with

$$k_1 = n_1 \frac{\omega_1}{c} \tag{4}$$

where n_1 is the refractive index of the material at the frequency ω_1, and c the velocity of light in vacuum. As we mentioned already, the input field will induce a polarization term at $\omega_2 = 2\omega_1$:

$$P[\omega_2] = \frac{1}{2}\epsilon_0 \chi^{(2)} A_1^2 \cos(2\omega_1 t - 2k_1 z) \tag{5}$$

As for the generated field E_2, it will propagate inside the crystal and can be described as

$$E_2 = A_2 \cos(\omega_2 t - k_2 z) = A_2 \cos(2\omega_1 t - k_2 z) \tag{6}$$

with

$$k_2 = \frac{n_2 \omega_2}{c} = \frac{n_2 \times 2\omega_1}{c} \tag{7}$$

Arguments of both cosine functions (eq. (6)) and eq. (3)) are identical if and only if $n_1 \equiv n_2$. As fig. 4 shows, dispersion prevents such equality[1]. We can introduce a *mismatch parameter* $\Delta k = k_2 - 2k_1$ and use it to write the *coherence length* ($L_{\text{coh.}}$) for second harmonic generation:

$$L_{\text{coh.}} = \frac{2\pi}{|\Delta k|} = \frac{2\pi}{\left| n_2 \frac{2\omega}{c} - 2 \frac{n_1 \omega}{c} \right|} = \frac{2\pi c}{2\omega} \frac{1}{|n_2 - n_1|} = \frac{\lambda}{2|n_2 - n_1|} \tag{8}$$

In the case of Franken & co-workers experiment, the coherence length was only a few micron!

[1]Realizing phase-matching will be the main topic of a separate chapter.

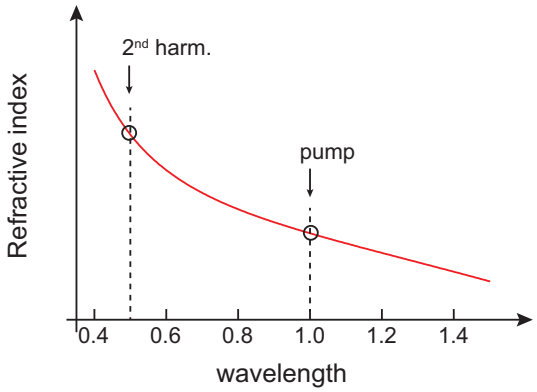

Figure 4: Evolution of the refractive index as a function of the wavelength.

0.1.3 General case

Let's assume that the experiment now focuses on sum-frequency generation. Two fields are required

$$E = E_1\ e^{i(\omega_1 t - \mathbf{k_1}\cdot\mathbf{r})} + E_2\ e^{i(\omega_2 t - \mathbf{k_1}\cdot\mathbf{r})} + c.c. \tag{9}$$

In this case, the fields are not necessarily co-linear. In the nonlinear polarization, the sum-frequency term will appear as

$$P = \epsilon_0 \chi^{(2)} \left[\cdots + E_1 E_2 e^{i(\omega_1+\omega_2)t - (\mathbf{k_1}+\mathbf{k_2})\cdot\mathbf{r}} + \ldots\right] \tag{10}$$

For the process to be efficient, we need to fulfill 2 conditions (fig. 5):

$$\omega_3 = \omega_1 + \omega_2 \quad \Rightarrow \quad \hbar\omega_3 = \hbar\omega_1 + \hbar\omega_2 \quad \text{(conservation of energy)} \tag{11a}$$
$$\mathbf{k_3} = \mathbf{k_1} + \mathbf{k_2} \quad \Rightarrow \quad \hbar\mathbf{k_3} = \hbar\mathbf{k_1} + \hbar\mathbf{k_2} \quad \text{(conservation of momentum)} \tag{11b}$$

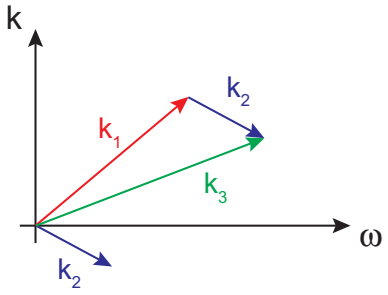

Figure 5: k *vs.* ω diagram for phase-matching

Usually, phase-matching requires the use of birefringence. For linear case (for instance inside a fiber), the phase-matching condition becomes simply

$$n_3\omega_3 = n_1\omega_1 + n_2\omega_2 \tag{12}$$

0.2 Second harmonic generation

First, we should state that as an incident field arrives on a $\chi^{(2)}$ crystal, the induced polarization $P_{\mathrm{NL}} = \epsilon_0\chi^{(2)}E^2$ will lead to the generation $E_{\mathrm{in}}(\omega) \rightarrow E(2\omega)$. And as soon as

this second harmonic exists and travels together with the fundamental we can have:

$$\begin{cases} \omega + 2\omega \\ 2\omega - \omega \\ \omega + \omega \\ 2\omega + 2\omega \to 4\omega \\ \dots \end{cases}$$

Starting at one frequency $m\omega$ (with $m = 1$) leads to the combination $1 + 2$ then $1 + 2 + 3 + \dots$. And the resulting polarization, in a very general form can be written as

$$P = \sum_m \tilde{P}[m\omega] = \sum_m \left[P(m\omega)e^{im\omega t} + c.c.\right] \tag{13}$$

Actually, all these higher harmonics ($m > 2$) do not need to be taken into account. This can be seen as using the *slow varying envelope approximation*: these frequencies oscillates far too fast to have any influence. In the case of second harmonic generation, where fundamental and second harmonic are co-propagating, we have the field

$$E = E_1\ e^{i\omega t} + E_2\ e^{2i\omega t} + c.c. \tag{14}$$

Then the optically induced polarization is

$$\begin{aligned} P =& \epsilon_0 \left[\chi^{(1)}E + \chi^{(2)}E^2\right] \\ =& \epsilon_0\chi^{(1)} \left[E_1\ e^{i\omega t} + E_2\ e^{2i\omega t} + c.c.\right] \\ &+ \epsilon_0\chi^{(2)} \left[E_1^2\ e^{2i\omega t} + \cancel{E_2^2\ e^{4i\omega t}} + \cancel{E_1E_2\ e^{3i\omega t}} + 2E_1E_2^*\ e^{-i\omega t} + c.c. + |E_1|^2 + |E_2|^2\right] \end{aligned}$$

Therefore, we can extract the polarization term oscillating a ω and 2ω:

$$\tilde{P}_{\text{lin.}}[\omega] = \epsilon_0\chi^{(1)}E_1e^{i\omega t} + c.c \tag{15a}$$

$$\tilde{P}_{\text{lin.}}[2\omega] = \epsilon_0\chi^{(1)}E_2e^{2i\omega t} + c.c \tag{15b}$$

$$\tilde{P}_{\text{NL}}[\omega] = P(\omega)e^{i\omega t} + c.c. = 2\epsilon_0\chi^{(2)}E_1^*E_2e^{i\omega t} + c.c. \tag{15c}$$

$$\tilde{P}_{\text{NL}}[2\omega] = P(2\omega)e^{2i\omega t} + c.c = \epsilon_0\chi^{(2)}E_1^2e^{2i\omega t} + c.c. \tag{15d}$$

And these terms are the driving terms for the propagation equation

$$\left[\partial_{zz} - \frac{1}{c^2}\partial_{tt}\right] E = \frac{1}{\epsilon_0 c^2}\partial_{tt}P \tag{16}$$

Obviously, the linear term (eq. (15a), (15b)) leads to the refractive index at the fundamental and the second harmonic:

$$n_m^2 = 1 + \chi^{(1)}(m\omega) \tag{17}$$

Similarly, we should isolate the contributions oscillating at $e^{j\omega t}$ and $e^{2j\omega t}$ resulting in

$$\left[\partial_{zz} - \frac{n_m^2}{c^2}\partial_{tt}\right] E_m = \frac{1}{\epsilon_0 c^2}\partial_{tt}\tilde{P}_{\text{NL}}(m\omega) \quad \text{with } m = 1, 2 \tag{18}$$

Introducing the spatial dependence of the electromagnetic field

$$E_m = A_m e^{-ik_m z} \qquad \text{where } k_m = \frac{n_m\omega_m}{c} = \frac{n_m \times m\omega}{c} \tag{19}$$

and assuming that the envelope A_m varies slowly over the the length $1/k_m$, the eq. (18) becomes

$$e^{-ik_m z}\left[\partial_{zz}A_m - 2ik_m\partial_z A_m - \frac{n_m^2}{c^2}\left(\partial_{tt}A_m + 2i\omega_m\partial_t A_m\right)\right] = \frac{1}{\epsilon_0 c^2}\left[\partial_{tt}P_{\mathrm{NL}}(m\omega) + 2i\omega_m\partial_t P_{\mathrm{NL}}(m\omega) - \omega_m^2 P_{\mathrm{NL}}(m\omega)\right] \tag{20}$$

We can then use the slow varying envelope approximation

$$\begin{cases} \partial_{zz}A_m - 2ik_m\partial_z A_m & \simeq -2ik_m\partial_z A_m \\ \partial_{tt}A_m + 2i\omega_m\partial_t A_m & \simeq 2i\omega_m\partial_t Am \\ \partial_{tt}P_{\mathrm{NL}} + 2i\omega_m\partial_t P_{\mathrm{NL}} - \omega_m^2 P_{\mathrm{NL}} & \simeq 2i\omega_m\partial_t P_{\mathrm{NL}} \simeq -\omega_m^2 P_{\mathrm{NL}} \end{cases}$$

Therefore for $m = 1$ the equation (18) becomes

$$e^{-ik_1 z}\left[-2ik_1\partial_z A_1 - 2i\frac{n_1^2}{c^2}\omega_1\partial_t A_1\right] = -\omega_1\frac{2\,\cancel{\epsilon_0}\,\chi^{(2)}}{\cancel{\epsilon_0}\,c^2}A_1^* A_2 e^{-i(k_2-k_1)z}$$

$$\Rightarrow \quad \boxed{\partial_z A_1 + \frac{n_1}{c}\partial_t A_1 = \frac{i\omega_1}{n_1\,c}\chi^{(2)}A_1^* A_2 e^{-i(k_2-2k_1)z}} \tag{21}$$

And similarly

$$\boxed{\partial_z A_2 + \frac{n_2}{c}\partial_t A_2 = \frac{i\omega_2}{2\,n_2\,c}\chi^{(2)}A_1^2 e^{+i(k_2-2k_1)z}} \tag{22}$$

At this stage, we need to distinguish between two very different situations (fig. 6).

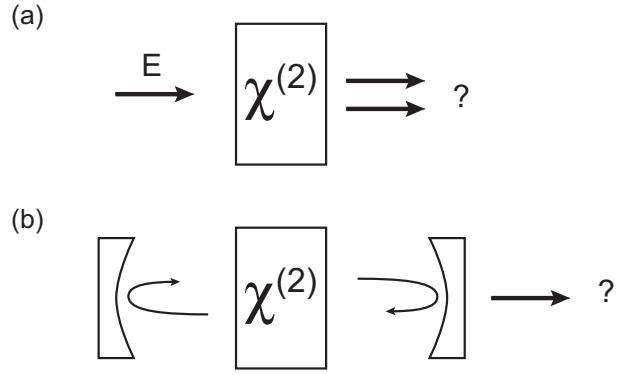

Figure 6: (a) free-running scheme and (b) scheme including a resonant cavity

In one case (fig. 6-a), the evolution of the pump and the generated signal happens along the crystal, but do not depend on the time. In such case the partial differentiation with respect to time $\partial_t A_m = 0$ in eq. (21) and (22) and these become a set of ordinary differential equations (eq. (23a), (23b)) In the other case, the full partial differential equations must be treated (eq. (21), (22)).

0.2.1 Free-running case

In the free-running case, the equations for the generation of second harmonic become a set of two coupled equations:

$$\frac{dA_1}{dz} = \frac{i\omega_1\chi^{(2)}}{n_1 c}A_1^* A_2 e^{-i\Delta kz} \tag{23a}$$

$$\frac{dA_2}{dz} = \frac{i\omega_2\chi^{(2)}}{2\ n_2 c}A_1^2 e^{+i\Delta kz} = \frac{i\omega_1\chi^{(2)}}{n_2 c}A_1^2 e^{+i\Delta kz} \tag{23b}$$

$$\text{with } \Delta k = k_2 - 2k_1$$

Obviously, the first option to deal with these equations is to solve them numerically using a good solver. This way could be simply named a *brute force approach* and usually does not really bring insight about the studied process. Looking a little closer, we can notice that

$$\frac{d\left|A_1\right|^2}{dz} = A_1^*\frac{dA_1^*}{dz} + A_1\frac{dA_1^*}{dz} = A_1^*\left[\frac{i\omega_1}{n_1\ c}\chi^{(2)}A_1^* A_2 e^{-i\Delta kz}\right] + A_1\left[\frac{-i\omega_1}{n_1\ c}\chi^{(2)}A_1 A_2^* e^{i\Delta kz}\right]$$

$$\Rightarrow\ \frac{d\left|A_1\right|^2}{dz} = \frac{i\omega_1}{n_1\ c}\chi^{(2)}\left[\ A_1^{*2}A_2 e^{-i\Delta kz} - A_1^2 A_2^* e^{i\Delta kz}\right] \tag{24}$$

$$\text{and for } A_2:\ \frac{d\left|A_2\right|^2}{dz} = \frac{i\omega_1}{n_2\ c}\chi^{(2)}\left[-A_1^{*2}A_2 e^{-i\Delta kz} + A_1^2 A_2^* e^{i\Delta kz}\right] \tag{25}$$

which leads to

$$n_1\frac{d\left|A_1\right|^2}{dz} + n_2\frac{d\left|A_2\right|^2}{dz} = 0 \tag{26}$$

This basically represents the conservation of the energy during the propagation. If we call J the energy flow, this quantity is constant and $n_1|A_1|^2 + n_2|A_2|^2 = J$. We can then express the amplitude of the field A_m as

$$A_m = \sqrt{\frac{J}{n_m}}\rho_m e^{i\phi_m} \tag{27}$$

and check that

$$\left.\begin{aligned} |A_1|^2 &= \frac{J}{n_1}\rho_1^2 \\ |A_2|^2 &= \frac{J}{n_2}\rho_2^2 \end{aligned}\right\} \Rightarrow \rho_1^2 + \rho_2^2 = 1 \tag{28}$$

Introducing eq. (27) into eq. (24) and (25) gives

$$\frac{d\rho_1}{dz} + i\rho_1\frac{d\phi_1}{dz} = \frac{i\omega_1\sqrt{J}}{n_1\ c\sqrt{n_2}}\chi^{(2)}\rho_1\rho_2\ e^{-i\Delta kz}e^{i(\phi_2 - 2\phi_1)} \tag{29a}$$

$$\frac{d\rho_2}{dz} + i\rho_2\frac{d\phi_2}{dz} = \frac{i\omega_1\sqrt{J}}{n_1\sqrt{n_2}\ c}\ \chi^{(2)}\rho_1^2\ e^{+i\Delta kz}e^{i(2\phi_1 - \phi_2)} \tag{29b}$$

Since the exponential has no dimension, we can extract from these equations a characteristic length ℓ and introduce the dimensionless propagation coordinate $\zeta = z/\ell$:

$$\ell = \frac{c\ n_1\sqrt{n_2}}{\omega_1\ \chi^{(2)}\sqrt{J}} \tag{30}$$

What is important to notice is that not only this characteristic length depends on the properties of the crystal ($n_1 = n(\omega_1)$, n_2 and $\chi^{(2)}$) but also on the used energy since $\sqrt{J}$ appears. Introducing the dimensionless propagation length $\zeta = z/\ell$ and the total phase mismatch $\theta = 2\phi_1 - \phi_2 + z\Delta k$, we get

$$\frac{d\rho_1}{d\zeta} + i\rho_1\frac{d\phi_1}{d\zeta} = i\rho_1\rho_2 e^{-i\theta} = i\rho_1\rho_2\left(\cos\theta - i\sin\theta\right) \tag{31a}$$

$$\frac{d\rho_2}{d\zeta} + i\rho_2\frac{d\phi_2}{d\zeta} = i\rho_1^2 e^{i\theta} = i\rho_1^2\left(\cos\theta + i\sin\theta\right) \tag{31b}$$

Separating real and imaginary parts of these equations will give the evolution of the amplitudes of each field ρ_m (real part) and total phase-mismatch (imaginary part). For the amplitudes:

$$d_\zeta\rho_1 = \rho_1\rho_2\sin\theta \tag{32a}$$

$$d_\zeta\rho_2 = -\rho_1^2\sin\theta \tag{32b}$$

and since $\theta = 2\phi_1 - \phi_2 + z\Delta k$, then[2] $d_\zeta\theta = 2d_\zeta\phi_1 - d_\zeta\phi_2 + \ell\Delta k$. And $d_\zeta\phi_m$ are given by the imaginary parts of the eq. (31a), and (31b):

$$\begin{cases} \rho_1 d_\zeta\phi_1 = \rho_1\rho_2\cos\theta \quad \Rightarrow \quad d_\zeta\phi_1 = \rho_2\cos\theta \\ \\ \rho_2 d_\zeta\phi_2 = \rho_1^2\cos\theta \quad \Rightarrow \quad d_\zeta\phi_2 = \left(\dfrac{\rho_1^2}{\rho_2}\right)\cos\theta \end{cases}$$

And finally:

$$\boxed{\begin{aligned} \frac{d\rho_1}{d\zeta} &= \rho_1\rho_2\sin\theta \qquad (33a)\\ \\ \frac{d\rho_2}{d\zeta} &= -\rho_1^2\sin\theta \qquad (33b)\\ \\ \frac{d\theta}{d\zeta} &= \left(2\rho_2 - \frac{\rho_1^2}{\rho_2}\right)\cos\theta + \ell\Delta k \qquad (33c) \end{aligned}}$$

0.2.2 Phase-matching or not...?

It is clear from the set of equations (eq. (33) that a few cases must be looked at, especially depending of the value of Δk.

Perfect phase-matching – $\Delta k = 0$

From the evolution of the phase θ, we can notice (see exercise):

$$\frac{d\theta}{d\zeta} = \left(2\rho_2 - \frac{\rho_1^2}{\rho_2}\right)\cos\theta \Longleftrightarrow \frac{d}{d\zeta}\left[\ln\left(\rho_1^2\rho_2\right)\cos\theta\right] = 0 \tag{34}$$

From Eq. (34), we find a second invariant

$$\rho_1^2\rho_2\cos\theta = G \tag{35}$$

Where G is a constant. G can either be null or not. For G to vanish, we have three cases: (i) $\rho_1 = 0$ (ii) $\rho_2 = 0$ or (iii) $\cos\theta = 0$.

[2]Remember that $\zeta = z/\ell$ and therefore $dz/d\zeta = \ell$!

- if $\rho_1 = 0$, then $\rho_2 = 1$ (because of eq. (28)). This would mean that only the second harmonic signal is at the entrance of the crystal. This would correspond to another process than second harmonic generation, since the conversion will now be from $2\omega \to \omega$, which is one form of *parametric down conversion*.
- if $\rho_2 = 0$, then all the energy at the entrance of the crystal is in the fundamental frequency ($\rho_1 = 1$). The evolution of ρ_2 requires that $\sin\theta < 0$ (see eq. (32b)), otherwise ρ_2 would decrease and become negative, which is not physical.
- if $\cos\theta = 0$ ... well, this will need to be looked at more carefully.

Imperfect phase-matching – $\Delta k \neq 0$

In the case of non-perfect phase-matching, and considering that $\rho_1^2\rho_2\cos\theta = G$ is a constant, we can notice that

$$\frac{d\theta}{d\zeta} = \left(2\rho_2 - \frac{\rho_1^2}{\rho_2}\right)\cos\theta + \ell\Delta k \Longleftrightarrow \frac{d}{d\zeta}\left(\rho_1^2\rho_2\cos\theta - \frac{\ell\Delta k}{2}\rho_2^2\right) = 0 \tag{36}$$

And therefore, as previously, we find another *invariant*

$$\rho_1^2\rho_2\cos\theta - \frac{\ell\Delta k}{2}\rho_2^2 = H \tag{37}$$

which is obviously equal to G in the case of perfect phase-matching $\Delta k = 0$. Finally, we have only three possibilities, that can lead to a non-null second harmonic generation:

- $\Delta k = 0$ and $G = 0$: we have perfect phase-matching.
- $\Delta k = 0$ and $G \neq 0$: there is already second harmonic at the entrance of the crystal. This is a seeded situation.
- $\Delta k \neq 0$

0.2.3 Perfect phase-matching and $G = 0$

The condition $G = 0$ requires $\cos\theta = 0$ and therefore $\theta = \pm\pi/2$. As discussed previously, for the second harmonic signal to grow, we must take $\sin\theta < 0$, and therefore must choose $\theta = -\pi/2$. The coupled equation (eq. (33)) then become:

$$\frac{d\rho_1}{d\zeta} = -\rho_1\rho 2 \tag{38a}$$

$$\frac{d\rho_2}{d\zeta} = +\rho_1^2 = 1 - \rho_2^2 \tag{38b}$$

Solution of eq. (38b) is simply $\tanh(\zeta + \zeta_0)$, which leads to $\rho_1(\zeta) = \mathrm{sech}(\zeta + \zeta_0)$. And to fix the initial condition, we can impose $\rho_2(\zeta = 0) = 0$, which immediately gives the solution

$$\rho_1(\zeta) = \mathrm{sech}(\zeta), \qquad \rho_2(\zeta) = \tanh(\zeta) \tag{39}$$

Remember that $\zeta = z/\ell$ and

$$\ell = \frac{n_1\sqrt{n2}}{\omega_1\chi^{(2)}}\frac{c}{\sqrt{J}} = \frac{\sqrt{n_1 n_2}}{\omega_1\chi^{(2)}}\frac{\epsilon_0 c}{|A_1(z=0)|}$$

From the non-dimensionless variables, we can extract the conversion efficiency of the second harmonic process:

$$\eta\left(\frac{z}{\ell}\right) = \left|\frac{A_2(z)}{A_1(0)}\right|^2 = \frac{(J/n_2)\,\rho_2^2\,(z/\ell)}{(J/n_1)\times 1} = \frac{n_1}{n_2}\tanh^2\left(\frac{z}{\ell}\right) \tag{40}$$

As we can see from this equation, it is not necessary to increase the propagation length inside a crystal to get a better conversion efficiency.

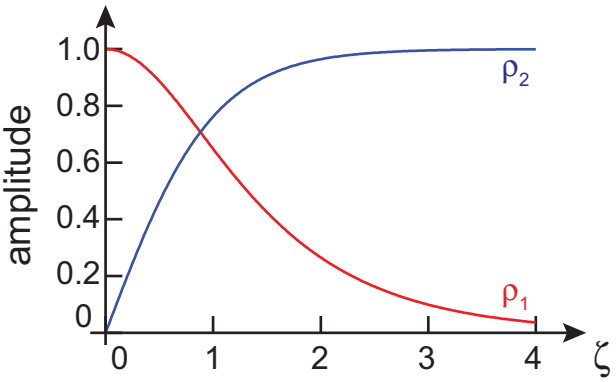

Figure 7: Evolution of the amplitude of the respectively the pump ρ_1 and the second harmonic ρ_2 as they are propagating inside the crystal. Initial condition is $\rho_1 = 1$, $\rho_2 = 0$, and $\theta = -\pi/2$ ($G = 0$).

0.2.4 Perfect phase-matching but $G \neq 0$

Since $\rho_1^2 \rho_2 \cos\theta = G$ and $\rho_1^2 + \rho_2^2 = 1$ then

$$\cos\theta = \frac{G}{\rho_1^2 \rho_2} = \frac{G}{\rho_2 \left(1 - \rho_2^2\right)} \tag{41}$$

Since $d_\zeta \rho_2^2 = 2\rho_2 d_\zeta \rho_2$, and using the evolution of ρ_2 (eq. (33b)) then

$$\frac{d\rho_2^2}{d\zeta} = +2\rho_2 \left(-\rho_1 \sin\theta\right) = \pm 2\rho_2 \rho_1^2 \sqrt{1 - \cos^2\theta} \tag{42}$$

Inserting eq. (41) leads to the evolution of the intensity of the second harmonic ρ_2^2:

$$\frac{d\rho_2^2}{d\zeta} = \pm 2\rho_2 \left(1 - \rho_2^2\right) \sqrt{1 - \frac{G^2}{\rho_2^2 \left(1 - \rho_2^2\right)^2}} = \pm 2\sqrt{\rho_2^2 \left(1 - \rho_2^2\right)^2 - G^2} \tag{43}$$

Such equation has a solution in terms of the Jacobi elliptic functions. The main point here is that the field amplitudes ρ_1 and ρ_2 will evolve periodically along the propagation.

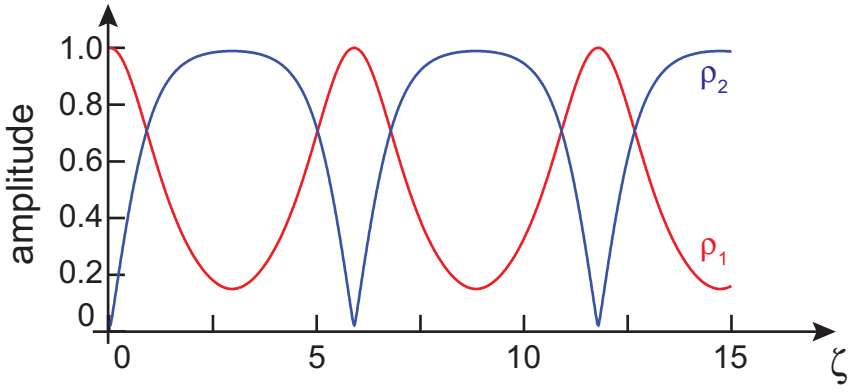

Figure 8: Evolution of the amplitude of the pump (ρ_1) and the second harmonic (ρ_2) as they are propagating inside the nonlinear crystal.

The two other parameters that we can modify are respectively the amount of pump (ρ_1) and the initial condition on the phase. Fig. 9 presents the evolution of the intensity of the second harmonic as a function of the initial parameters, respectively the input pump for a fixed phase (fig. 9.a), and the influence of the input phase for a fixed input pump energy.

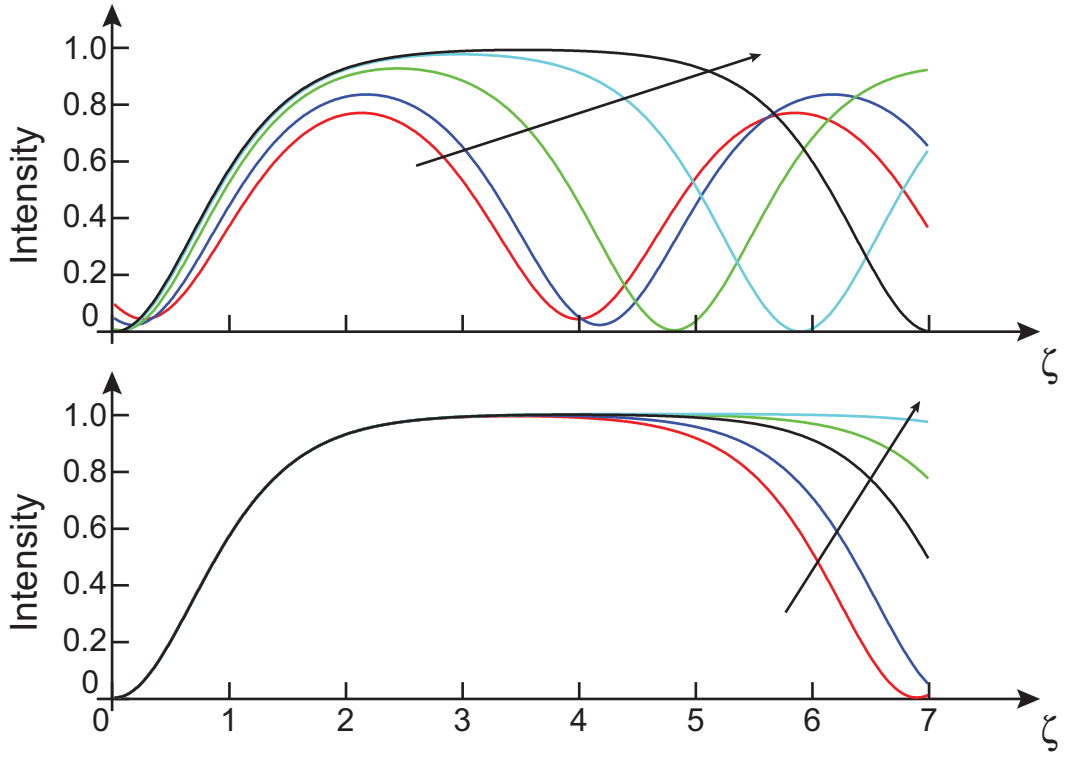

Figure 9: Evolution of the intensity second harmonic (ρ_2^2) for a fixed pump power as a function of the initial pump amplitude (a) and the initial phase condition (b). For (a), the initial conditions are $\theta = \pi/4$ and $\rho_1 = 0.9$, 0.95, 0.99 and 0.999 (increase as the arrow) and for (b) $\rho_1^2(0) = 0.9999$ and $\theta = 2\pi/10$, $3\pi/10$, $4\pi/10$, $4.4\pi/10$ and $4.8\pi/10$.

0.2.5 Imperfect phase-matching

As we did previously, using the conservation of energy $\rho_1^2 + \rho_2^2 = 1$ and the invariant H (eq. (37)) we can derive the evolution of the intensity along the propagation:

$$\frac{d\rho_2^2}{d\zeta} = \pm 2\rho_2 \left(1 - \rho_2^2\right) \sqrt{1 - \cos^2\theta} = \pm 2 \sqrt{\rho_2^2 \left(1 - \rho_2^2\right)^2 - \left(H + \frac{1}{2}\ell \Delta k \rho_2^2\right)^2} \tag{44}$$

As before, and although the increased degree of complexity of the equation, the solution could also be expressed in terms of Jacobi elliptic function. The evolution of pump and second harmonic are, as previously, periodically changing along the propagation.

It is clear that fulfilling the phase-matching conditions is a crucial point to achieve a good conversion from the pump to the second harmonic. From two fields, we saw (see. p.2) that several different combinations can lead to different new frequency, each of them requiring a specific phase-matching. What was applied here in the specific case of second harmonic generation could also be transposed to any of these cases (sum-frequency, difference frequency... etc).

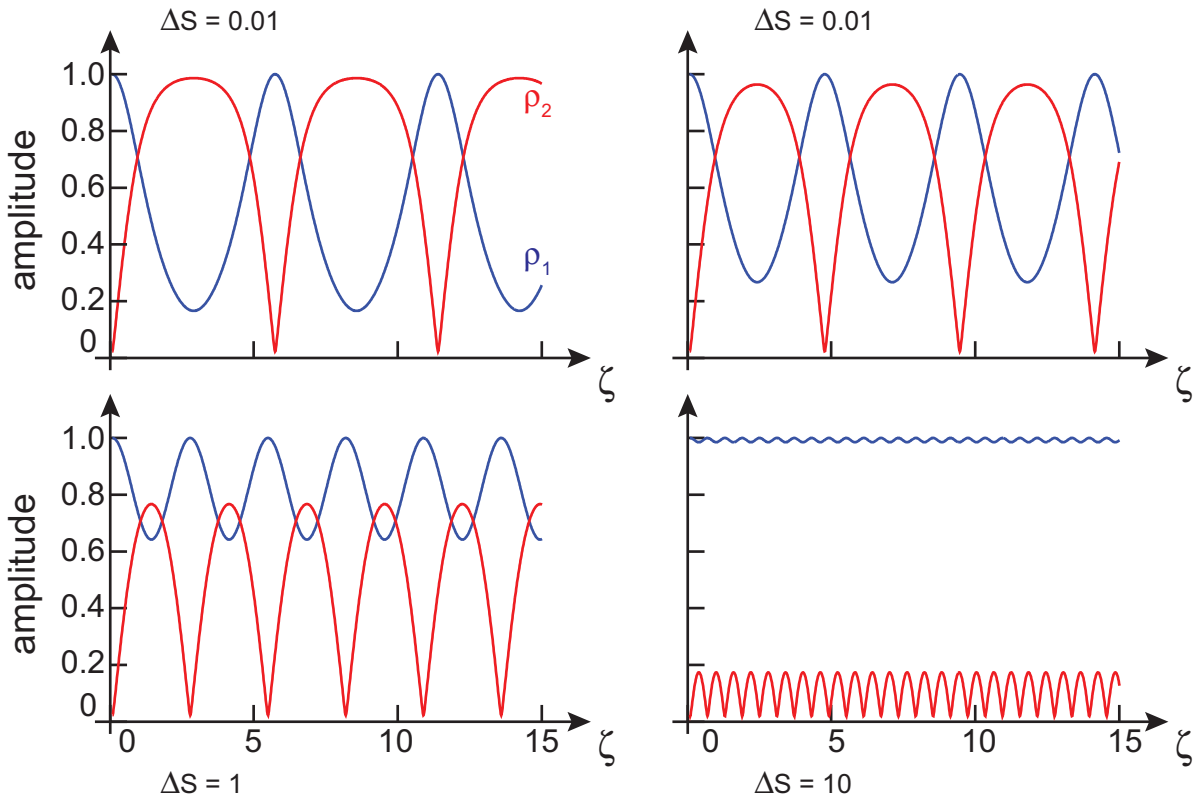

Figure 10: Evolution of the amplitudes (ρ_1 and ρ_2) as a function of the phase mismatch $\Delta S = \ell \Delta k$. Input conditions are $\rho_1^2(0) = 0.99$ and $\theta = \pi/4$.

0.2.6 Low depletion case

Let consider that the limit case when the pump is weakly depleted. The evolution of the second harmonic is them simply given by

$$\frac{dA_2}{dz} = \frac{i\omega_1}{n_2 c}\chi^{(2)} A_1^2 e^{iz\cdot\Delta k}$$
$$\Rightarrow \quad A_2(z) = \frac{\omega_1}{n_2 c}\chi^{(2)} A_1^2 \frac{e^{iz\cdot\Delta k} - 1}{\Delta k} \qquad \left(\times \frac{z}{z}\right)$$

and therefore the intensity evolves as

$$|A_2(z)|^2 = \left[\frac{\omega_1 \chi^{(2)}}{n_2 c}\, z\right]^2 |A_1|^4 \left[\frac{\sin(z\cdot\Delta k/2)}{(z\cdot\Delta k/2)}\right]^2 \tag{45}$$

Since the intensity if linked to the amplitude of the electric field by

$$I_i = \frac{1}{2} n_i c \epsilon_0 |A_i|^2 \tag{46}$$

we can rewrite eq. (45) as

$$I_2 = \frac{1}{2} n_2 c \epsilon_0 \left[\frac{\omega_1 \chi^{(2)}}{n_2 c}\, z\right]^2 \times \frac{4}{n_1^2 c^2 \epsilon^2} |I_1|^2 \,\mathrm{sinc}^2\left(\frac{z\cdot\Delta k}{2}\right)$$

$$\Rightarrow \quad \boxed{I_2(z) = \frac{2\left(\omega_1 \chi^{(2)}\right)^2}{n_1^2 n_2 c^3 \epsilon_0} z^2 I_1^2 \,\mathrm{sinc}^2\left(\frac{z\cdot\Delta k}{2}\right)} \tag{47}$$

Since the *sinc* function has its maximum at $z \cdot \Delta k = 0$, and minima periodically spread at $(z \cdot \Delta k / 2) = p\pi$ with $p \in \mathbb{Z}^*$. The first minimum of this function ($z \cdot \Delta k = 2p\pi$) corresponds to the coherence length:

$$z = \frac{2\pi}{\Delta k} = L_{\text{coh.}} \tag{48}$$

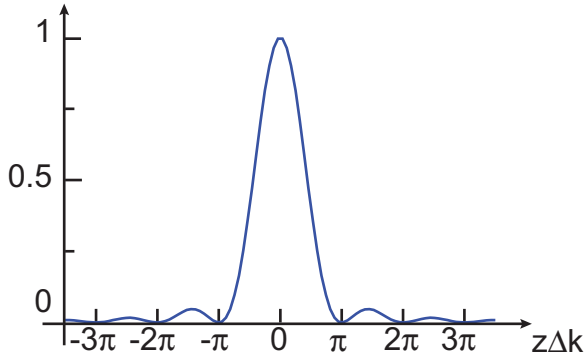

Figure 11: Sine cardinal and its first zeros.

Finally, from eq. (**??**) we can deduce the conversion efficiency:

$$\eta(z) = \left| \frac{A_2(z)}{A_1(0)} \right|^2 = \left(\frac{z\omega_1}{n_2 c} \chi^{(2)} |A_1(0)| \right)^2 \text{sinc}^2 \left(\frac{z\Delta k}{2} \right) \tag{49}$$

If we work at the phase-matching ($z\Delta k = 0$), then the sine cardinal is simply one, and we see that the conversion efficiency $\eta \propto |A_1(0)|^2$. Note also that the conversion efficiency increases with ω_1: it is easier to achieve second harmonic in the visible than in the infrared!

For perfect phase-matching ($\Delta k = 0$) the conversion efficiency scales as z^2. By contrast, when phase-matching is not fulfilled the conversion efficiency periodically oscillate (fig.). We have not discussed yet how to achieve phase-matching, but since we are using $\chi^{(2)}$ material, which are non-centrosymmetric crystal, we can imagine to grow one type of nonlinear crystal over one coherence length, and then another type (with reverse sign of Δk) so that the conversion efficiency carries on increasing along the propagation length. This idea of reversing the orientation of the crystal every coherence length is called *quasi-phase-matching* (QPM).

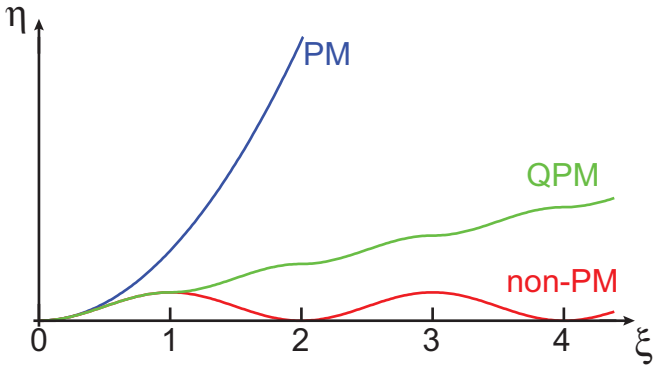

Figure 12: conversion efficiency (η) of the second harmonic process for non-phase-matched (red), perfectly phase-matched (blue) and quasi-phase-matched (green) conditions as a function of the length $\xi = z/L_{\text{coh.}}$.

0.2.7 Three waves mixing – Generalization

The natural generalization of second harmonic process is the sum-frequency generation: two fields oscillating respectively at ω_1 and ω_2 interact inside a $\chi^{(2)}$ crystal to generate a third wave oscillating at $\omega_3 = \omega_1 + \omega_2$. The total field inside the medium is a superposition of the three waves:

$$E(t) = E_1 e^{i\omega_1 t} + E_2 e^{i\omega_2 t} + E_3 e^{i\omega_3 t} + c.c.$$

As for the case of second harmonic, we should (i) calculate the nonlinear polarization $P_{\mathrm{NL}} = \epsilon_0 \chi^{(2)} E^2$ and then introduce it into the propagation equation

$$\partial_{zz} E_m - \frac{n_m^2}{c^2} \partial_{tt} E_m = \frac{1}{\epsilon_0 c^2} \partial_{tt} P(m\omega)$$

Using similar approach than for the second harmonic process, we can then derive the set of coupled equations:

$$\begin{cases} \left(\partial_z + \dfrac{n_1}{c}\partial_t\right) A_1 &= \dfrac{i\omega_1}{n_1 c}\chi^{(2)} A_2^* A_3 e^{iz\Delta k} \\ \left(\partial_z + \dfrac{n_2}{c}\partial_t\right) A_2 &= \dfrac{i\omega_2}{n_2 c}\chi^{(2)} A_1^* A_3 e^{iz\Delta k} \\ \left(\partial_z + \dfrac{n_3}{c}\partial_t\right) A_3 &= \dfrac{i\omega_3}{n_3 c}\chi^{(2)} A_1 A_2 e^{-iz\Delta k} \\ \Delta k &= k_3 - k_1 - k_2 \end{cases} \tag{50}$$

and in the case of free-running situation (no cavity), $\partial_t A_i = 0$. Therefore we have

$$\begin{cases} \dfrac{dA_1}{dz} &= \dfrac{i\omega_1}{n_1 c}\chi^{(2)} A_2^* A_3 e^{iz\Delta k} \\ \dfrac{dA_2}{dz} &= \dfrac{i\omega_2}{n_2 c}\chi^{(2)} A_1^* A_3 e^{iz\Delta k} \\ \dfrac{dA_3}{dz} &= \dfrac{i\omega_3}{n_3 c}\chi^{(2)} A_1 A_2 e^{-iz\Delta k} \end{cases} \tag{51}$$

As previously, we can use $n_1 d_z |A_1|^2 = n_1 \left(A_1 d_z A_1^* + A_1^* d_z A_1\right)$, then

$$\begin{cases} n_1 \dfrac{d|A_1|^2}{dz} &= \omega_1 \dfrac{i\chi^{(2)}}{c}\left(A_1^* A_2^* A_3 e^{iz\Delta k} - A_1 A_2 A_3^* e^{-iz\Delta k}\right) \\ n_2 \dfrac{d|A_2|^2}{dz} &= \omega_2 \dfrac{i\chi^{(2)}}{c}\left(A_1^* A_2^* A_3 e^{iz\Delta k} - A_1 A_2 A_3^* e^{-iz\Delta k}\right) \\ n_3 \dfrac{d|A_3|^2}{dz} &= -\omega_3 \underbrace{\dfrac{i\chi^{(2)}}{c}\left(A_1^* A_2^* A_3 e^{iz\Delta k} - A_1 A_2 A_3^* e^{-iz\Delta k}\right)}_{\varphi} \end{cases} \tag{52}$$

Since $\omega_1 + \omega_2 = \omega_3$, we see that

$$\begin{aligned} & n_1 d_z |A_1|^2 + n_2 d_z |A_2|^2 = -n_3 d_z |A_3|^2 \\ \Rightarrow\ & d_z \left(n_1 |A_1|^2 + n_2 |A_2|^2 + n_3 |A_3|^2\right) = 0 \end{aligned} \tag{53}$$

As for the second harmonic process we find that the conservation of energy leads to $n_1|A_1|^2 + n_2|A_2|^2 + n_3|A_3|^2 = J$, where J is a constant. We can also notice from eq. (52) that $\varphi = ({}^{n_1}/_{\omega_1})\, d_z|A_1|^2 = ({}^{n_2}/_{\omega_2})\, d_z|A_2|^2 = -({}^{n_3}/_{\omega_3})\, d_z|A_3|^2$. As previously, we can use the complex notation for the amplitude

$$A_m = \sqrt{J\,\frac{\omega_m}{n_m}}\rho_m e^{i\phi_m} \tag{54}$$

and notice that

$$\begin{aligned}
d_z\left(\frac{n_1}{\omega_1}|A_1|^2 - \frac{n_2}{\omega_2}|A_2|^2\right) &= 0 = d_z J_1 \\
d_z\left(\frac{n_2}{\omega_2}|A_2|^2 + \frac{n_3}{\omega_3}|A_3|^2\right) &= 0 = d_z J_2 \\
d_z\left(\frac{n_1}{\omega_1}|A_1|^2 + \frac{n_3}{\omega_3}|A_3|^2\right) &= 0 = d_z J_3
\end{aligned}$$

Therefore

$$\begin{aligned}
& J_1 = \frac{n_1}{\omega_1}|A_1|^2 - \frac{n_2}{\omega_2}|A_2|^2 \\
\Rightarrow\ & J_1 = \frac{n_1}{\omega_1}\left(J\,\frac{\omega_1}{n_1}\rho_1^2\right) - \frac{n_2}{\omega_2}\left(J\frac{\omega_2}{n_2}\rho_2^2\right) \\
\Rightarrow\ & \frac{J_1}{J} = \rho_1^2 - \rho_2^2 \quad \text{is invariant}
\end{aligned}$$

Similarly, $\rho_1^2 + \rho_3^2 = {}^{J_3}/_{J}$ and $\rho_2^2 + \rho_3^2 = {}^{J_2}/_{J}$.

Using the definition of the amplitude A_m in the set of equations (eq. (52)) then leads to the generalized set of coupled equations for three wave interaction:

$$\frac{d\rho_1}{d\zeta} = -\rho_2\rho_3\sin\theta \tag{55a}$$

$$\frac{d\rho_2}{d\zeta} = -\rho_3\rho_1\sin\theta \tag{55b}$$

$$\frac{d\rho_3}{d\zeta} = \rho_1\rho_2\sin\theta \tag{55c}$$

$$\frac{d\theta}{d\zeta} = \left(\frac{\rho_1\rho_2}{\rho_3} - \frac{\rho_1\rho_3}{\rho_2} - \frac{\rho_2\rho_3}{\rho_1}\right)\cos\theta + \ell\Delta k \tag{55d}$$

We can notice that if we are in the degenerate case, where $E_1 = E_2$ ($\rho_1 = \rho_2$), we find immediately the equations for the second harmonic (eq. (33)).

0.2.8 How to achieve phase-matching for $\chi^{(2)}$ process?

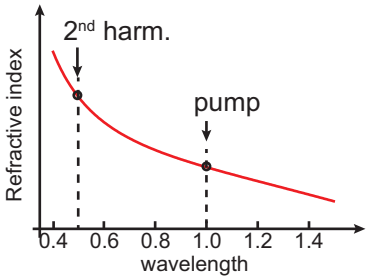

As we have already discussed, the dispersion of the material prevent the direct phase-matching between the fundamental frequency and its second harmonic. Indeed the phase matching conditions and energy conservation are simply

$$\left\{ \begin{array}{rcl} 2\omega_p &=& \omega_s \\ 2k_p &=& k_s \end{array} \right. \Rightarrow \frac{2n(\omega_p)}{c}\,\omega_p = \frac{n(\omega_s)}{c}\,\omega_s$$

The main idea to achieve phase-matching is to utilize anisotropy of crystals. From Maxwell's equations, we can write

$$\left. \begin{array}{rcl} \nabla \times \mathbf{H} &=& \partial_t \mathbf{D} \quad \Rightarrow \quad j\mathbf{k}\times\mathbf{H} = j\omega\mathbf{D} \quad \Rightarrow \quad \mathbf{k}\perp\mathbf{D} \text{ and } \mathbf{H}\perp\mathbf{D} \\ \nabla \times \mathbf{E} &=& -\partial_t \mathbf{B} \quad \Rightarrow \quad j\mathbf{k}\times\mathbf{E} = -i\omega\mathbf{B} \quad \Rightarrow \quad \mathbf{k}\perp\mathbf{B} \text{ and } \mathbf{E}\perp\mathbf{B} \end{array} \right\} \Rightarrow \mathbf{E} \in (0, \mathbf{D}, \mathbf{k})$$

Obviously, $\mathbf{E} \in (0, \mathbf{k}, \mathbf{D})$ does not necessarily imply that $\mathbf{k} \perp \mathbf{E}$! Note that this also implies that the Poynting vector $\mathbf{S} = \mathbf{E} \times \mathbf{H}$ is not necessarily co-linear with $\mathbf{k}$. In a general form the displacement is

$$\mathbf{D} = \epsilon_0 \mathbf{E} + \mathbf{P} = \epsilon_0 \hat{\epsilon}_r \mathbf{E} \tag{56}$$

where $\hat{\epsilon}_r$ is a tensor. For nonmagnetic and transparent material, $\hat{\epsilon}_r$ is symmetric and can be diagonalized such that

$$\mathbf{D} = \epsilon_0 \begin{bmatrix} \epsilon_1 & \dots & \\ \vdots & \epsilon_2 & \\ & & \epsilon_3 \end{bmatrix} \begin{pmatrix} E_x \\ E_y \\ E_z \end{pmatrix} = \epsilon_0 \begin{bmatrix} n_x^2 & \dots & \\ \vdots & n_y^2 & \\ & & n_z^2 \end{bmatrix} \begin{pmatrix} E_x \\ E_y \\ E_z \end{pmatrix} \tag{57}$$

The eigenvector of $\hat{\epsilon}_r$ are the *principal* axis of the crystal. Three cases are possible depending of the respective values of n_i:

- if $n_x = n_y = n_z$, then we have an *isotropic* material
- if $n_x = n_y \neq n_z$, the crystal is said to be *uniaxial*
- if $n_x \neq n_y \neq n_z$, the crystal is *biaxial*

Ellipsoid of indices

Using the well-know algebraic relationship $\nabla \times \nabla \times \mathbf{E} = \nabla(\nabla.\mathbf{E}) - \nabla^2\mathbf{E}$ on Maxwell's equations give the relationship

$$\mathbf{D} = \frac{1}{\mu_0\omega^2}\left[\mathbf{k}^2\mathbf{E} - \mathbf{k}(\mathbf{k}\cdot\mathbf{E})\right] \tag{58}$$

and using the relationship (eq. (57)) then this equation becomes

$$\mathbf{k}(\mathbf{k}\cdot\mathbf{E}) = \mathbf{k}^2\mathbf{E} - \mu_0\epsilon_0\omega^2 \begin{bmatrix} n_x^2 & & \\ & n_y^2 & \\ & & n_z^2 \end{bmatrix} \mathbf{E}$$

$$\begin{aligned} \text{and} \quad \mathbf{k}(\mathbf{k}\cdot\mathbf{E}) &= (k_x\hat{\mathbf{e}}_x + k_y\hat{\mathbf{e}}_y + k_z\hat{\mathbf{e}}_z)(k_xE_x + k_yE_y + k_zE_z) \\ &= k_x^2E_x\hat{\mathbf{e}}_x + k_xk_yEy\hat{\mathbf{e}}_x + k_xk_yE_z\hat{\mathbf{e}}_x \\ &+ k_xk_yE_x\hat{\mathbf{e}}_y + k_y^2Ey\hat{\mathbf{e}}_y + k_yk_zE_z\hat{\mathbf{e}}_y \\ &+ k_xk_zE_x\hat{\mathbf{e}}_z + k_yk_zEy\hat{\mathbf{e}}_z + k_z^2E_z\hat{\mathbf{e}}_z \end{aligned}$$

Projecting on the principal axis, we get

$$
\begin{aligned}
/x \rightarrow \quad & \left(k_y^2 + k_z^2 - \mu_0\epsilon_0\omega^2 n_x^2\right) E_x &&= k_x k_y E_y + k_x k_z E_z \\
/y \rightarrow \quad & \left(k_x^2 + k_z^2 - \frac{n_y^2\omega^2}{c^2}\right) E_y &&= k_x k_y E_x + k_y k_z E_z \\
/z \rightarrow \quad & \left(k_x^2 + k_y^2 - \frac{n_z^2\omega^2}{c^2}\right) E_z &&= k_x k_z E_x + k_y k_z E_y
\end{aligned}
$$

and this can be rewritten as

$$
\begin{cases}
\left(k_y^2 + k_z^2 - \frac{n_x^2\omega^2}{c^2}\right) E_x & -k_x k_y E_y & -k_x k_z E_z & = 0 \\
-k_x k_y E_x & \left(k_x^2 + k_z^2 - \frac{n_y^2\omega^2}{c^2}\right) E_y & -k_y k_z E_z & = 0 \\
-k_x k_z E_x & -k_y k_z E_y & \left(k_x^2 + k_y^2 - \frac{n_z^2\omega^2}{c^2}\right) E_z & = 0
\end{cases} \tag{59}
$$

This set of coupled equations can only have solution if $\det|\ldots| = 0$. After some calculations we can write this determinant as

$$
-\frac{\omega^4}{c^4} + \frac{\omega^2}{c^2}\left(\frac{k_y^2 + k_z^2}{n_x^2} + \frac{k_x^2 + k_z^2}{n_y^2} + \frac{k_x^2 + k_y^2}{n_z^2}\right) + \left(\frac{k_x^2}{n_y^2 n_z^2} + \frac{k_y^2}{n_x^2 n_z^2} + \frac{k_z^2}{n_x^2 n_y^2}\right)|k|^2 = 0 \tag{60}
$$

This surface can be simplified in the case of uniaxial crystal. In this case $n_x = n_y = n_o$ the ordinary index, and $n_z = n_e$ is the extraordinary axis. The surface (eq. (60)) becomes

$$
\underbrace{\left(\frac{k_x^2 + k_y^2 + k_z^2}{n_o^2} - \frac{\omega^2}{c^2}\right)}_{\text{sphere}}\underbrace{\left(\frac{k_x^2 + k_y^2}{n_e^2} + \frac{k_z^2}{n_o^2} - \frac{\omega^2}{c^2}\right)}_{\text{ellipsoid}} = 0 \tag{61}
$$

To represent these two surface more easily, we draw only a cut at $x = 0$. Two cases are possible depending of the sign of $n_e - n_o$: The direction corresponding to the contact

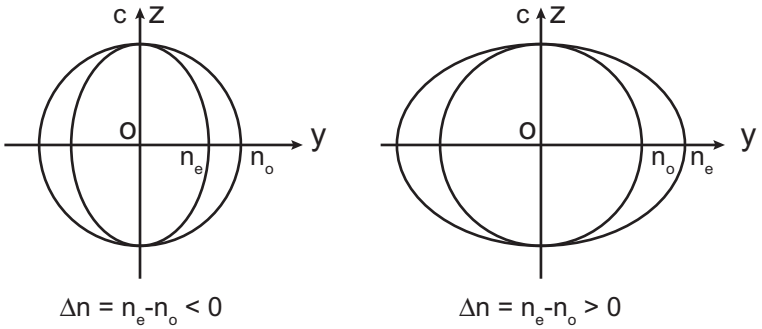

Figure 13: Refractive indices for the case of negative ($\Delta n = n_e - n_o < 0$) and positive uniaxial crystals.

between the sphere and the ellipsoid is called the *optical axis*, and is denoted as **c**. Along this axis, the wave propagates with <u>one</u> phase velocity since there is only one refractive index. In the general case (biaxial crystal) the situation is obviously more complex and there are two directions with equal phase velocity.

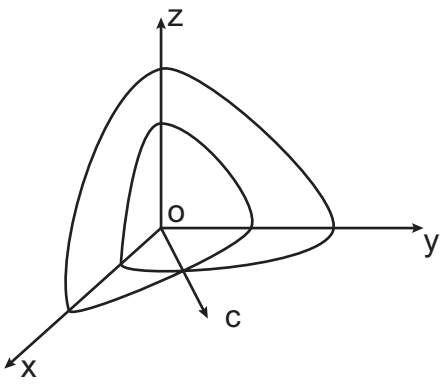

Figure 14: Refractive indices for a biaxial crystal.

Use of double-refraction to achieve phase-matching

The easiest way to understand the principle of double-refraction due to the birefringence of a crystal is to simply draw the construction for the refraction of a beam randomly polarized (fig. 15). As we can see, both polarization get separated as the beam is refracted. We are

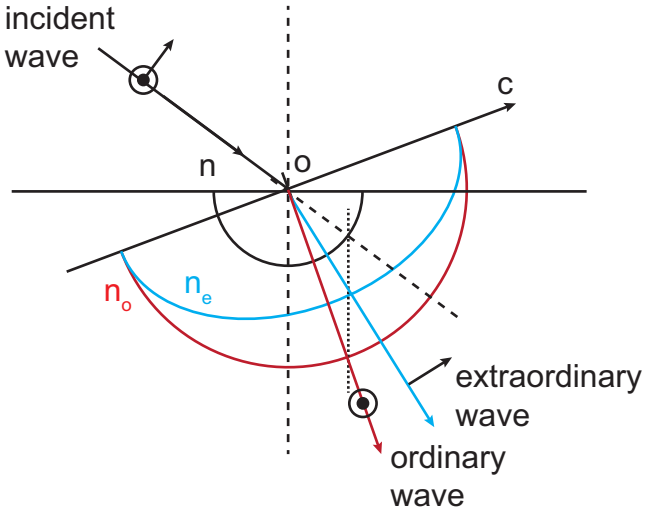

Figure 15: Fresnel construction for the refraction of a beam inside a negative crystal, where the optical axis **c** does not coincide with the surface.

going to use this effect to achieve phase-matching.

Let us first consider the sum-frequency generation (SFG) in the particular case of negative uniaxial crystal. Two types of phase-matching conditions are possible, whether the initial waves are both in the same polarization or not. In the first case (type-I phase-matching) the generated wave will be polarized orthogonal to the input waves:

$$k_{o1} + k_{o2} = k_3^e(\theta) \tag{62a}$$

$$k_1^e(\theta) + k_2^e(\theta) = k_{3o} \tag{62b}$$

In short notation, we can write this as $o + o \rightarrow e$ or simply (ooe), corresponding to negative crystal, and $e + e \rightarrow o$ or *eeo* for positive crystals. By contrast, for *type-II* phase-matching, we mix two orthogonal polarization in order to generate the third wave. Then several cases are possible. For negative crystals:

$$k_{o1} + k_2^{(e)}(\theta) = k_3^{(e)}(\theta) \qquad o + e \rightarrow e$$

$$k_1^{(e)}(\theta) + k_{o2} = k_3^{(e)}(\theta) \qquad e + o \rightarrow e$$

and for positive crystals:

$$k_{o1} + k_2^{(e)}(\theta) = k_{o3} \qquad o + e \to o$$
$$k_1^{(e)}(\theta) + k_{o2} = k_{o3} \qquad e + o \to o$$

Fig. 16 shows how to find the direction of collinear phase-matching for type-I SHG in an uniaxial negative crystal.

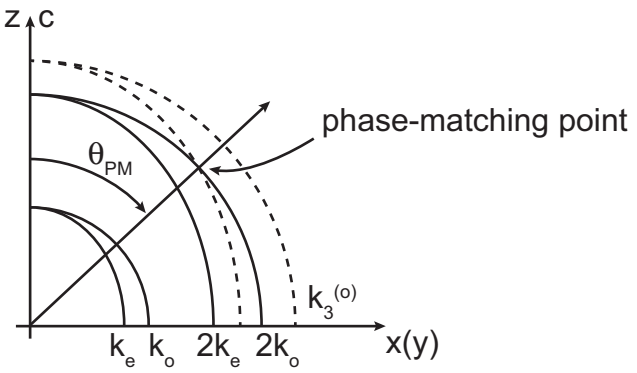

Figure 16: Phase-matching condition for the case of a negative uniaxial crystal

Obviously, we cannot list everything here. This depends on the situation, the crystal used... etc. In general, most cases are non-colinear (type-II) phase-matching, but in practice people tend to use type-I. For uniaxial crystals, the phase-matching angle can be calculated using the table 1:

Negative uniaxial crystal	Positive uniaxial crystal
$\tan^2\theta_{\rm pm}^{ooe} = \dfrac{1-U}{W-1}$	$\tan^2\theta_{\rm pm}^{eeo} \simeq \dfrac{1-U}{U-S}$
$\tan^2\theta_{\rm pm}^{eoe} \simeq \dfrac{1-U}{W-R}$	$\tan^2\theta_{\rm pm}^{oeo} = \dfrac{1-V}{V-Y}$
$\tan^2\theta_{\rm pm}^{oee} \simeq \dfrac{1-U}{W-Q}$	$\tan^2\theta_{\rm pm}^{eoo} = \dfrac{1-T}{T-Z}$

Table 1: Equations for calculating the phase-matching angle in the case of uniaxial crystals - from ref. [2].

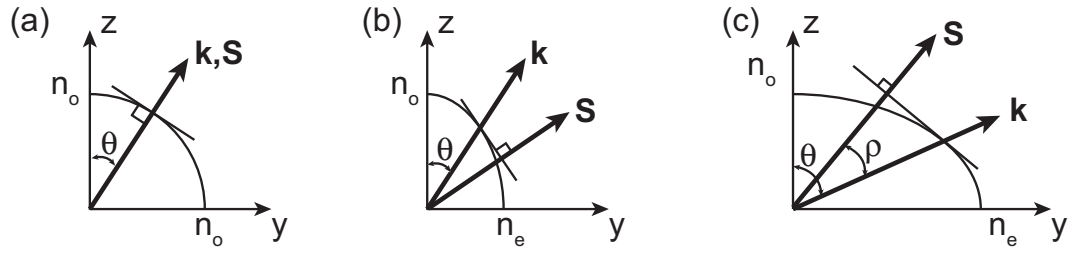

Figure 17: Disposition of the wave vector (**k**) and the Poynting vector **S** in an isotropic medium (a), and a negative (b) and positive (c) birefringent uniaxial crystal. ρ is the anisotropy angle.

with

$$U = \frac{(A+B)^2}{C^2} \quad W = \frac{(A+B)^2}{F^2} \quad R = \frac{(A+B)^2}{(D+B)^2}$$

$$Q = \frac{(A+B)^2}{(A+E)^2} \quad S = \frac{(A+B)^2}{(D+E)^2} \quad V = \frac{B^2}{(C-A)^2}$$

$$Y = \frac{B^2}{E^2} \qquad T = \frac{A^2}{(C-B)^2} \qquad Z = \frac{A^2}{D^2}$$

$$A = \frac{n_{o1}}{\lambda_1} \qquad B = \frac{n_{o2}}{\lambda_2} \qquad C = \frac{n_{o3}}{\lambda_3}$$

$$D = \frac{n_{e1}}{\lambda_1} \qquad E = \frac{n_{e2}}{\lambda_2} \qquad F = \frac{n_{e3}}{\lambda_3}$$

Note that this table is established for the general case $\mathbf{k}_1 + \mathbf{k}_2 \rightarrow \mathbf{k}_3$. Therefore for second harmonic these equations simplify since $A = B$ and $D = E$.

0.2.9 Walk-Off

When a wave propagates inside a *uniaxial* crystal, the direction of the propagation of the phase (**k**) generally does not coincide with the direction of Poynting vector **S**, which characterizes he direction of propagation of the energy. The direction of **S** can be defined as the normal to the tangent drawn at the point of intersection of vector **k** with the curve $n(\theta)$. For ordinary wave, the normal to the tangent coincides with the wave vector **k**, so the phase and the energy of the wave propagate in the same direction (Fig. 17a). For an extraordinary wave, situation of very different as the normal to this tangent does not coincide with the wave vector **k** (Fig. 17 b,c). In this case, the energy in the extraordinary beam slips away from the axis of the ordinary beam: this is the *walk-off*.

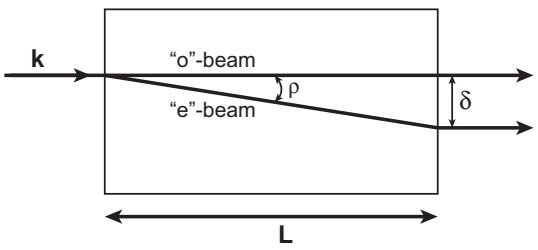

Figure 18: Walk-off of an extraordinary wave, with respect to the ordinary beam.

The *walk-off* angle ρ is

$$\rho(\theta) = \pm \tan^{-1}\left[\left(\frac{n_o}{n_e}\right)^2 \tan\theta\right] \mp \theta \tag{63}$$

where the upper signs refer to a negative crystal and the lower ones to a positive one.

0.2.10 Optical parametric amplifier

As an example for the use of a nonlinear crystal, we describe here the setup of an optical parametric amplifier (OPA). This equipment allows to generate tunable pulses from fs-pulses emitted by a Ti:Sa laser system ($\lambda = 800$ nm). About 25% of the incident beam is focused into a sapphire crystal in order to generate white light. This will be then combined with the rest of the 800 nm-pump inside a BBO crystal. Moreover in oder to maximize the conversion efficiency, the generated signal/idler are sent back inside the BBO crystal with the leftover pump. For this the overlap between generated signal and pump must be carefully adjusted, and this is the reason of both delay lines in the setup. Finally signal and idler as well as the residual pump are separated by dichroic mirror.

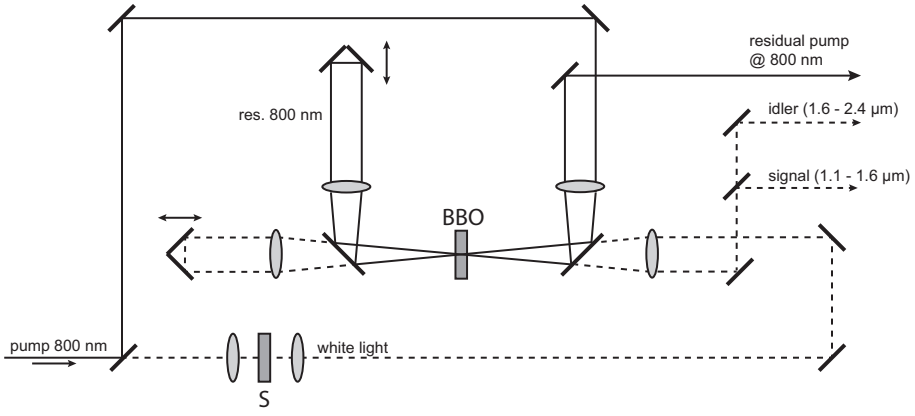

Figure 19: Schematic of an optical parametric amplifier.

0.3 Second harmonic with Gaussian beam

So far we always wrote the electric field as

$$E = E_1 e^{i\omega_1 t} + E_2 e^{i\omega_2 t} + c.c \tag{64}$$

With such a form, not only we only consider that the we have continuous wave (E_i = constant) but also this corresponds to a plane wave! In reality nonlinear optics requires high electric field and it is therefore important to focused tightly the beam (Gaussian) inside the crystal but also use pulsed-laser. Here, we will focus on practical consideration resulting in the *walk-off* of the beam and also how to optimize the conversion using focused beam. Note however that we will assume that the pulse are long enough so that the dispersion effects can be neglected.

0.3.1 Use of Gaussian beam

We remind that for a Gaussian beam we can describe the electric field as:

$$E(\mathbf{r},t) = \frac{1}{2}E_0(\omega)\frac{w_0}{w(z)}\exp\left[i\left(kz + \psi(z) - \omega t\right) - \frac{r^2}{w^2(z)} + i\frac{kr^2}{2R(z)}\right] \tag{65}$$

with

$$\text{radius of curvature} : R(z) = z\left[1 + \left(\frac{Z_R}{z}\right)^2\right] \tag{66a}$$

$$\text{Rayleigh length} : Z_R = \frac{\pi w_0^2}{\lambda} = \frac{\pi w_0^2 n(\omega)}{\lambda_{\text{vac.}}} \tag{66b}$$

$$\text{waist} : w^2(z) = w_0^2\left[1 + \left(\frac{z}{Z_R}\right)^2\right] \tag{66c}$$

$$\text{the divergence} : \theta_{\text{div.}} = \frac{w_0}{Z_R} = \frac{\lambda}{\pi w_0} \tag{66d}$$

$$\text{and the Gouy phase} : \psi(z) = \text{atan}\left(\frac{z}{Z_R}\right) \tag{66e}$$

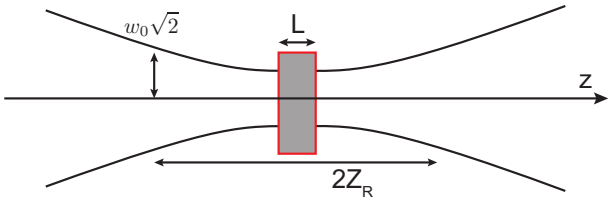

Figure 20: Gaussian beam focused inside a nonlinear material

It is clear from the figure 20, that the conversion efficiency will greatly depend on the length of the crystal with respect to the confocal parameter ($2Z_R$) over which the beam can be considered as collimated.

case 1: $L \ll Z_R$

This case corresponds to large crystals. The radius of curvature of the phase front can be considered as constant and large. We can therefore consider that the beam is like as plane-wave, with limited boundaries, and diffraction can be neglected.

The input energy is[3]

$$I(\mathbf{r},\omega) = I(0,\omega)\exp\left(-\frac{2r^2}{w_0^2(\omega)}\right) \tag{67}$$

Actually what is important is the power:

$$P(\omega) = I(0,\omega)\int_0^{2\pi} d\theta \int_0^{\infty} \exp\left(-\frac{2r^2}{w_0^2}\right) r dr \tag{68a}$$

$$P(\omega) = \frac{\pi w_0^2}{2} I(0,\omega) \tag{68b}$$

For simplicity, we take the case of type-I (*eoo*), perfect phase-matching ($\Delta k = 0$) and low depletion of the pump. Assuming that the field varies slowly over one wavelength, the second harmonic can be described as:

$$E(\mathbf{r},t) = \frac{1}{2}A_2(z,r,2\omega)\exp\left[i\left(2\omega t - 2k(\omega)z\right)\right] + c.c. \tag{69}$$

The amplitudes of the pump and the second harmonic evolve following the eq. (23b)

$$d_z A_2 = \frac{i\omega_1}{n_2 c}\chi^{(2)} E_0^2(\omega)\exp\left[-\frac{2r^2}{w_0^2(\omega)}\right] \tag{70}$$

and this needs to be integrated over the whole length of the crystal L, leading to

$$\begin{aligned} E(L,r,2\omega) &= \frac{i\omega_1}{n_2 c}\chi^{(2)} E_0^2(\omega)\exp\left[-\frac{2r^2}{w_0^2(\omega)}\right]\int_0^L dz \\ &= \frac{i\omega_1}{n_2 c}\chi^{(2)} E_0^2(\omega)\exp\left[-\frac{2r^2}{w_0^2(\omega)}\right] L \end{aligned} \tag{71a}$$

If you compare eq. (71a) and eq. (65) you can notice that the generated beam has a smaller diameter:

$$w_0(2\omega) = \frac{w_0(\omega)}{\sqrt{2}} \tag{72}$$

Note that this is a general feature when harmonic is generated: **the output beam is narrowed is space!**

Rayleigh length?

The generated beam diameter being narrower than the pump beam, it perfectly makes sense to wonder about the Rayleigh length of the generated beam. Let's write the Rayleigh length at the new frequency:

$$Z_R(2\omega) = \frac{\pi w_0^2(2\omega) n(2\omega)}{\lambda_{\text{vac.}}(2\omega)} = \frac{\pi\left(\frac{w_0^2(\omega)}{2}\right) n(2\omega)}{\left(\frac{\lambda_{\text{vac.}}}{2}\right)} = \frac{\pi w_0^2(\omega) n(2\omega)}{\lambda_{\text{vac.}}} \simeq Z_R(\omega) \tag{73}$$

The last sign ($\simeq$) assumes that $n(\omega) \simeq n(2\omega)$, which is obviously correct since we are working at perfect phase matching. Although the beam is narrower, its Rayleigh length is the same than the one of the pump. Its divergence however is larger!

[3]We remind that the intensity of the beam is linked with the amplitude of the electric field by

$$I(0,\omega) = \frac{1}{2}c\epsilon_0 n(\omega)\left|E_0(\omega)\right|^2$$

Total power?

Actually, the total power is certainly what matters the most. To calculate this quantity, we must integrate over the whole beam:

$$\begin{aligned}
P(2\omega) &= \iint I(L,r,d\theta) r dr d\theta \\
&= \frac{1}{2} n_2 c \epsilon_0 \left| \frac{\omega_1}{n_2 c} \chi^{(2)} E_0^2(\omega) \right|^2 L^2 \iint \exp\left(-\frac{4r^2}{w_0^2(\omega)} \right) r dr d\theta \\
&= \frac{1}{2} n_2 c \epsilon_0 \left| \frac{\omega_1}{n_2 c} \chi^{(2)} E_0^2(\omega) \right|^2 L^2 \int_0^{2\pi} d\theta \int_0^{\infty} \exp\left(-\frac{4r^2}{w_0^2(\omega)} \right) r dr \\
P(2\omega) &= \frac{1}{2} \frac{\left(\omega_1 \chi^{(2)} L\right)^2}{n_2 c} \frac{\pi w_0^2(\omega)}{4} |E_0(\omega)|^4
\end{aligned}$$

And since we have the input power

$$\begin{aligned}
P(\omega) &= \frac{\pi w_0^2}{2} I(0,\omega) = \frac{\pi w_0^2}{2} \times \frac{1}{2} n_1 c \epsilon_0 |E_0|^2 \\
\Rightarrow \quad |E_0|^2 &= \frac{4P(\omega)}{\pi w_0^2 n_1 c \epsilon_0}
\end{aligned}$$

Finally the conversion efficiency is

$$\frac{P(2\omega)}{P(\omega)} = \frac{2\left(\omega_1 \chi^{(2)} L\right)^2}{n_1^2 n_2 c^3 \epsilon_0 \pi w_0^2} P(\omega) \tag{76}$$

case 2: $L \approx Z_R$ (optimum case)

This case is obviously more difficult since the diffraction of the beam can no longer be ignored. Of course, we can always think that a tight focusing will improve the conversion efficiency since the density of power will be higher, but in that case the confocal parameter ($2Z_R$) would also be reduced, reducing the efficient interaction length. It is therefore **not** obvious where the optimum would be.

As before, let assume that we have a crystal cut for type-I (*eoo*) phase-matching and that we operate at perfect phase matching ($\Delta k = 0$). We also assume that the birefringence is small. In this case the total power of the generated second harmonic is given by[4]

$$P(2\omega) = \frac{1}{2} n_2 c \epsilon_0 \left| \frac{\omega_1 \chi^{(2)}}{2 n_2 c} E_0^2 \right|^2 \int_0^{2\pi} d\theta \int_0^{\infty} \left[\int_{-L/2}^{+L/2} \frac{w_0^2(\omega)}{w^2(z,\omega)} \exp\left(-\frac{2r^2}{w^2(z,\omega)} \right) dz \right]^2 r dr \tag{77}$$

G.D.Boyd and co-worker[5] studied carefully this problem and introduced a function $h_0(\xi)$, where $\xi = {}^{L}/_{(2Z_R)}$. The detail of the integration are "*hidden*" in the function $h_0(\xi)$, which is plotted on fig. 21. Using $h_0(\xi)$ the conversion efficiency can be written as

$$\frac{P(2\omega)}{P(\omega)} \simeq \frac{\left(\omega_1 \chi^{(2)}\right)^2}{n_1^2 n_2 c^3 \epsilon_0 \ \lambda_{\text{vac.}}(\omega_1)} \ h_0(\xi) L P(\omega) \tag{78}$$

[4] we assume here that the beam waist is located in the middle of the crystal.

[5] For more information, refer to G.D.Boyd and D.A. Kleinman, J. Appl. Phys. **39** p. 3597 (1968).

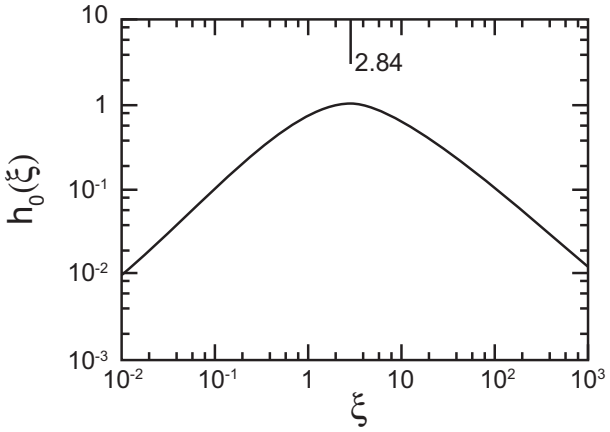

Figure 21: The function $h_0(\xi)$ as a function of ξ. Reproduced from G.D.Boyd and D.A. Kleinman, J.Appl.Phys. **39** p. 3597 (1968).

0.3.2 Use of pulsed laser

Since nonlinear effects require high intensities, many nonlinear experiments are done with pulsed lasers. For instance, first generation of second harmonic was done as soon as Q-switched laser were available. Let then assume that we use a pulse at the input beam. Since we are not only interesting in the power that we will generate, and we would not be able to resolve fast dynamical change of the power, we can simply describe the time-dependent power as

$$P(\omega, t) = P(\omega) e^{-2t^2/\tau^2(\omega)} \tag{79}$$

Obviously using eq. (79) to write the time-dependent power at the second harmonic we have

$$P(2\omega, t) \propto P^2(\omega, t) = P(2\omega) \underbrace{\exp\left(-\frac{4t^2}{\tau^2(\omega)}\right)}_{\rightarrow\ \tau(2\omega)=\dfrac{\tau(\omega)}{\sqrt{2}}} \tag{80}$$

As for the spatial case, the second harmonic is compressed in time in comparison with the input field.

General comment Nonlinear interaction will lead to compression if both space and time. The higher the order of the nonlinearity, the stronger the compression.

Since we are more or less interested only by the pulse energy $\Delta E = \int_{-\infty}^{+\infty} P(\omega_i, t) dt$ we can readily write the energy of the second harmonic by using eq. (80):

$$\Delta E(2\omega) = \sqrt{\frac{\pi}{4}}\, \tau(\omega) P(2\omega, 0) \tag{81}$$

Combining the temporal and spatial dependence yields (for $L \ll 2Z_R$)

$$\frac{\Delta E(2\omega)}{\Delta E^2(\omega)} = \frac{1}{\sqrt{\pi}\ \tau(\omega)} \left(\frac{P(2\omega, 0)}{P^2(\omega, 0)}\right) = \frac{\left(\omega_1\ \chi^{(3)} L\right)^2}{2\pi^{3/2}\ n_1^2 n_2\ c^3 \epsilon_0\ w_0^2\ \tau(\omega)} \tag{82}$$

0.3.3 Walk-off of Gaussian beam.

As the beam propagates inside the crytal, due to the critical angle necessary to achieve perfect phase matching there is always a walk-off between the pump and the generated

beam. We have already discussed this point for the case of plane-wave. In that case, the walk-off does not imply any degradation of the conversion efficiency. Obviously for real beam the limited size of the beam is rather incompatible with a good conversion efficiency of the second harmonic since the conversion requires an overlap between fundamental and harmonic. For thick crystal, the generation is then distributed along the transverse axis (Fig 22) and the conversion efficiency drops as we will see.

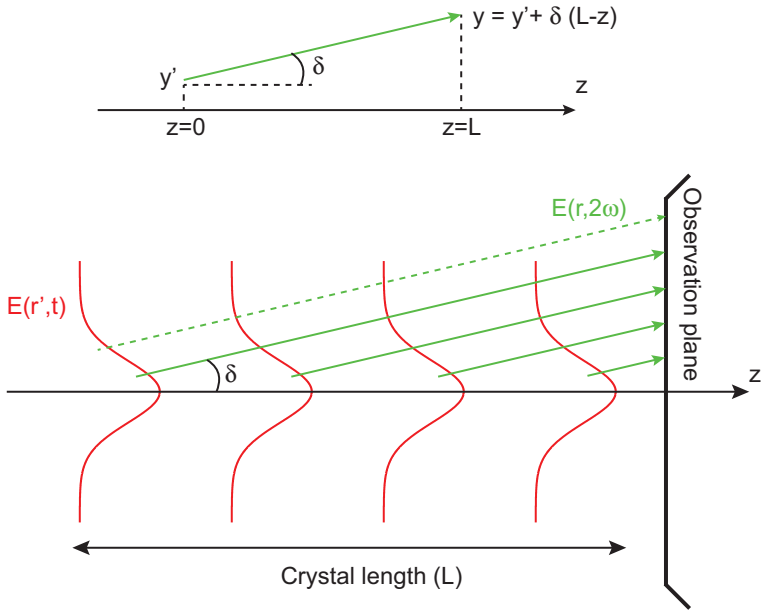

Figure 22: Walk-off between the fundamental and the harmonic in a type-I second harmonic generation (*ooe*) at the critical angle phase matching.

We take the case of type-I conversion (*ooe*), and we assume that the diffraction is limited ($w(z) \simeq w_0$). The fundamental field is

$$\mathcal{E}(z', \omega, x', y') \simeq \mathcal{E}_0^2(\omega) \exp\left[-\frac{(x'^2 + y'^2)}{w_0^2(\omega)}\right] \tag{83}$$

After the crystal, the harmonic field is

$$\mathcal{E}(L, 2\omega, x, y) \simeq i\frac{\omega_1 \chi^{(2)}}{2n_2 c}\mathcal{E}_0^2(\omega) \int_0^L \exp\left\{-\frac{2\left[x^2 + (y - \delta(L-z))^2\right]}{w_0^2(\omega)}\right\} dz \tag{84}$$

To integrate properly this equation, it is necessary to proceed a few change of variables:

$$u = \sqrt{2}\frac{y - \delta L}{w_0(\omega)}, \quad \xi = \sqrt{2}\frac{z\delta}{w_0(\omega)}, \quad \zeta = \sqrt{2}\frac{\delta L}{w_0(\omega)}, \quad F(u, \xi) = \frac{1}{\zeta}\int_0^\zeta e^{-(u+\xi)^2} d\xi \tag{85}$$

This then yields

$$\mathcal{E}(L, 2\omega) \simeq i\frac{\omega_1 \chi^{(2)}}{2n_2 c} L\mathcal{E}_0^2 \exp\left(-\frac{2x^2}{w_0^2(\omega)}\right) F(u, \zeta) \tag{86}$$

The function $F(u, \zeta)$ describes the influence of the walk-off. Fig. 23 shows the norm of this function $|F(u, \zeta)|^2$ for various values of ζ. This parameter ζ essential reflects the amount of walk-off to the harmonic beam radius.

As shown on fig. 23, the larger the walk-off relative to the original beam radius (larger ζ), the smaller the conversion efficiency, but also the more diffuse is the generated beam

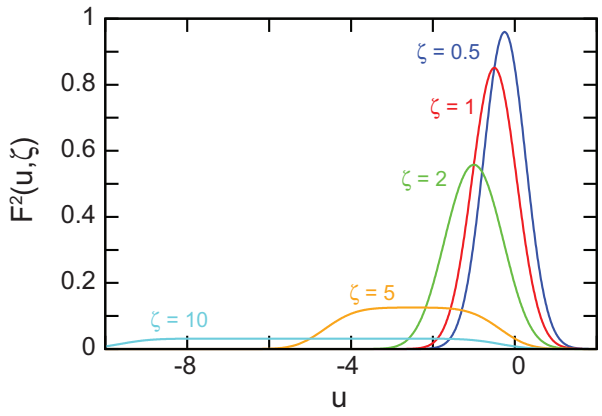

Figure 23: Beam profile obtained along the y-axis due to walk-off for various values of ζ. [Reproduced from G.D. Boyd *et al.*, Phys. Rev. **137** 1305 (1965)]

along the y-axis. Of course both are undesirable characteristics. The reduction of the total second harmonic generated can be quantified as

$$G(\zeta) = \sqrt{\frac{2}{\pi}} \int_{-\infty}^{+\infty} F^2(u,\zeta)du \;\rightarrow\; \frac{P(2\omega)}{P(\omega)} = \frac{\left(\omega_1 L \chi^{(2)}\right)^2}{2\pi w_0^2(\omega)\ \epsilon_0 c^3 n_2 n_1^2} G(\zeta) P(\omega) \qquad (87)$$

The function $G(\zeta)$ is plotted on Fig.xxx as a function of $\zeta' = \sqrt{2\pi}L/\ell_{wo}$, where $\ell_{wo} = \sqrt{\pi}\,[w_0(\omega)/\delta]$ is the walk-off length. As depicted by the plot of $G(\zeta)$ to keep the conversion efficiency above 50% it is important that $\zeta' \leq 3$.

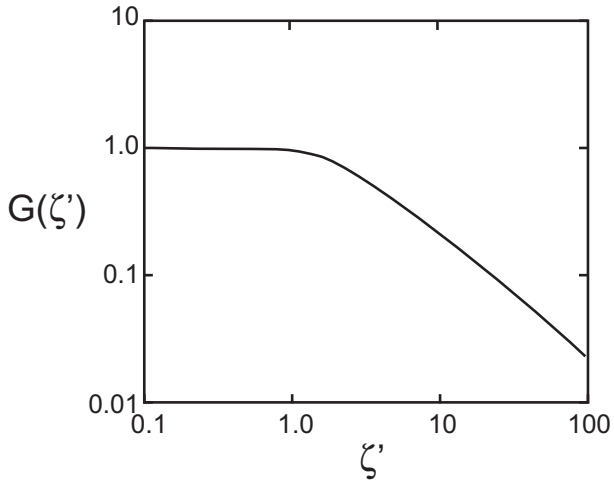

Figure 24: Decrease of the total second harmonic as a function of the ratio of the beam walk-off to the beam propagation distance of the fundamental beam. [Reproduced from G.D. Boyd *et al.*, Phys. Rev. **137** 1305 (1965)]

.1 Appendices

.1.1 Construction of the refracted beam

We remind here how to construct the refracted beam from a bean incident onto a surface S with an angle i. Of course, we can use Snell's law, but the goal here is to construct the beam in an easy way without calculating the refracted angle. The natural way is to use the *Huygens' construction*. Suppose that we have a plane wave incident onto a surface, separating two media. Their respective refractive index is n_1 and n_2. The plane wave Σ_0 arrives at the surface with a angle i_1 (fig. 26). In each medium, the phase velocity $v_{\phi i}$ is directly related to the refractive index by c/n_i.

Remember that the Huygens' hypothesis is that as the light propagate, each point from the plane wave is a source for a spherical wave, and the envelope of all these spherical surface is also a plane wave.

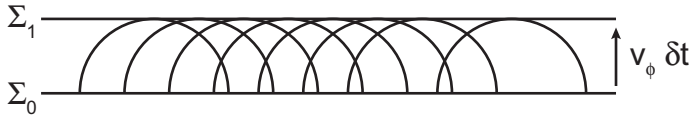

Figure 25: Huygens hypothesis for the propagation of a plane wave, travelling a phase-velocity v_ϕ.

The plane wave Σ_0 arrive in J locate at a distance $v_{\phi 1}\delta t$. In the second medium, the plane-wave Σ_2 is the envelope of the sphere with a radius

$$r = v_{\phi 2}\delta t$$

Since J belong to both surfaces Σ_1 and Σ_2, we see that Σ_2 is obtained by drawing the tangent to the circle with a radius $v_{\phi 2}$ and passing through J. And the direction of the refracted beam is orthogonal to Σ_2. Of course, from this construction, we can retrieve

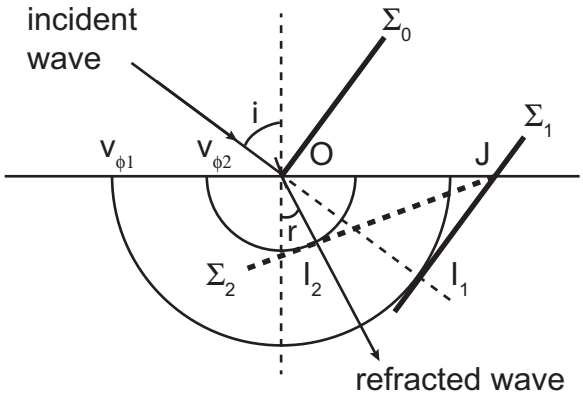

Figure 26: Huygens construction to draw the refracted beam of any beam incident on a surface with an angle i.

easily the Snell's law, since

$$OI_1 = OJ\sin i \qquad \text{and} \qquad OI_2 = OJ\sin r$$

Therefore

$$\frac{OI_1}{OI_2} = \frac{n_2}{n_1} = \frac{\sin i}{\sin r}$$

Another construction, which obviously gives the very same result. This time, instead of drawing circle with radius corresponding to the phase-velocities, we draw circle with radius n_i. The center of the circle is still the point of entrance of the beam.

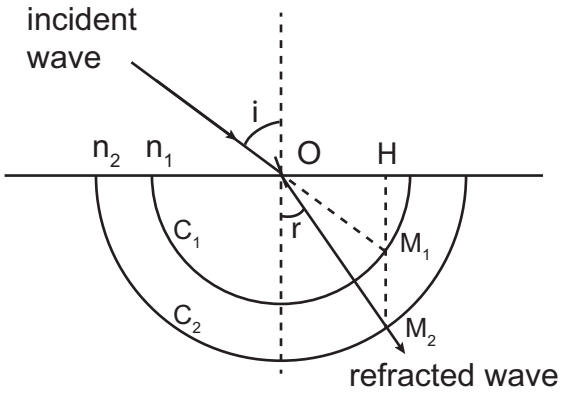

Figure 27: Construction of the refracted beam using the circle C_i of radius n_i.

Construction : We extend the incident beam up to M_1 the crossing with the circle C_1. We then project onto the second circle C_2. The refracted beam is simply OM_2. In this case, it is obvious that the distance OH can either be expressed as $n_1 \sin i$ or as $n_2 \sin r$, which leads to Snell's law again.

Bibliography

[1] Robert Boyd. *Nonlinear OPtics*. Academic Press, 2008.

[2] V.G. Dmitriev, G.G. Gurzadyan, and D.N. Nikogosyan. *Handbook of Nonlinear Optical Crystals*. Springer-Verlag, 1991.

[3] Paul Mandel. *Nonlinear Optics*. Wiley-VCH Verlag GmbH, 2010.

[4] Geoffrey New. *Introduction to nonlinear optics*. Cambridge University Press, 2011.

[5] G.I. Stegeman and R.A. Stegeman. *Nonlinear Optics*. John Wiley & Sons, Inc., 2012.